



THE EVALUATION OF METHODS FOR IMPROVING BEAMFORMING MAPS IN NOISY ENVIRONMENT

Jeoffrey Fischer¹ and Con Doolan¹

¹UNSW Sydney

High St Kensington, NSW 2052, Sydney, Australia

Abstract

This paper evaluates two novel methods to improve frequency-domain beamforming source location in noisy and reverberant environments. Experiments have been carried out with a speaker placed in an anechoic wind tunnel behind a flow generated by a noisy fan. The first method is based on a filtering of the cross-correlation matrix between each pair of microphones, i.e. the time-domain equivalent of the cross-spectral matrix. Indeed, as the source of interest (speaker) and the contaminating sources (fan) are far from each other, their signature in the cross-correlation functions can be separated. This method has already been validated in a reverberant environment, but the results obtained in the present case were not conclusive. Thus another method based on an eigenvalue decomposition was used to investigate the problem of high background noise in wind tunnel testings.

1 INTRODUCTION

Acoustic measurements during wind tunnel testings are difficult, for two main reasons: first, the test-section is usually hard-walled, which causes the noise to be multiply reflected. Second, the flow is generated by a fan which can, in some cases, be much louder than the source of interest. These issues can be solved experimentally, by installing acoustic foam covered with perforated plates in the test section and also by adding a muffler in the tunnel to reduce the fan noise. But these procedures are time and money consuming, that is why post-processing methods are often preferred.

The problem of reflections in acoustic maps has been first investigated by Guidati et al. [6] in the case of a rectangular test section. The positions of the image sources due to the wall were estimated theoretically and their effect was incorporated into the beamforming process. When applying this so-called reflection canceller on experimental trailing edge noise, the beamforming map was better resolved. This method has been recently used by other authors [2, 3] and

is now known as the Image Source Method (ISM). Fischer and Doolan [4] have compared the results obtained with this numerical method with an experimentally measured Green's function and showed that the resolution of the main peak showed more improvement with the experimental steering vectors rather than with the ISM. Another approach was proposed by Sijtsma and Holthusen [8] where the beamforming algorithm was modified to take into account the influence of a mirror source coherent with the main peak and lead to a better estimation of the focused beamformer spectra.

A recent method has been proposed by Fischer and Doolan [5] to solve this particular problem, and will be tested in this paper. Dereverberation Beamforming (DBF) is based on a filtering of the cross-correlation matrix (obtained from the usual cross-spectral matrix) in order to remove the influence of noise sources that reach the microphones with a different time-delay than the source of interest. DBF has already been validated in a reverberant test-section and it was demonstrated that the method greatly improves the location of the source compared to Conventional beamforming (CBF). In addition, the resolution of the main lobe was found to be comparable with the Point Spread Function (PSF), which makes it a very efficient method. Only the level could not be properly recovered.

High background noise issues have also been a focus of interest over the last decades. Koop and Ehrenfried [7] have compared several denoising methods including a wavenumber representation where the background noise caused by the fan is assumed to propagate in plane waves and thus can be removed in the beamforming algorithm. Another option is to measure the background noise while performing the array measurement so that it can be filtered out using an Adaptive Noise Canceller [9]. More recently, Bahr and Horne [1] have proposed to use Eigenvalue Decomposition (EVD) on the background noise Cross-Spectral Matrix (CSM) in order to recover the source CSM using some operators. It was then possible to recover sound source locations with very small Signal to Noise Ratio (SNR).

This paper presents the results of a systematic evaluation of DBF and EVF in a high background noise environment.

2 EXPERIMENTAL SETUP

The experiment were conducted in the Anechoic Wind-Tunnel (AWT) of the aerospace laboratory at UNSW Sydney. The open jet has a section of $0.46 \text{ m} \times 0.46 \text{ m}$. A 64-channel acoustic array was set on one side of the flow, which was run at $U_\infty = 20 \text{ m/s}$. The array has a multi-arm logarithmic design and is composed of 7 arms with 9 microphones in each plus one additional microphone in the center. The inner and outer radii of the spiral are respectively 0.9 m and 1.5 m. Each 1/4" GRAS 40PH phase matched microphone (frequency range [50 Hz ; 10 kHz]) was connected to a PXIe-4499 24 bit simultaneous sample computer. Actually, the microphones are sensitive to 20 kHz but beyond 10 kHz the gain of the frequency response is not constant. The 64 microphones are fixed on a perforated plate so that the design of the array can be adapted to different test cases. The plate is mounted on two stands and can be rotated to allow vertical and horizontal measurements when necessary. This design allows more flexibility for future acoustic array measurements. A ReSponse speaker located on the other side of the flow was used as a noise source (the speaker) and uses a white noise signal as an input. The speaker was run at several levels ranging from 1% to 100% of its capacity. The source-array distance is $L = 1 \text{ m}$. The complete setup is displayed in Figure 1. The recording parameters used here

are the same as for the previous experiment, except for the signal duration which was set to $T = 32$ s here.

The different spectra obtained with the speaker alone are shown and compared with the background noise from the fan in Fig.2. The different levels at which the speaker was run are shown here. Note that the SNR varies between positive and negative values, ranging from +25 dB down to -45 dB.



Figure 1: Experimental setup of the microphone array (left) and the speaker (right) in the anechoic wind tunnel. The test section (flow inlet) is located in between.

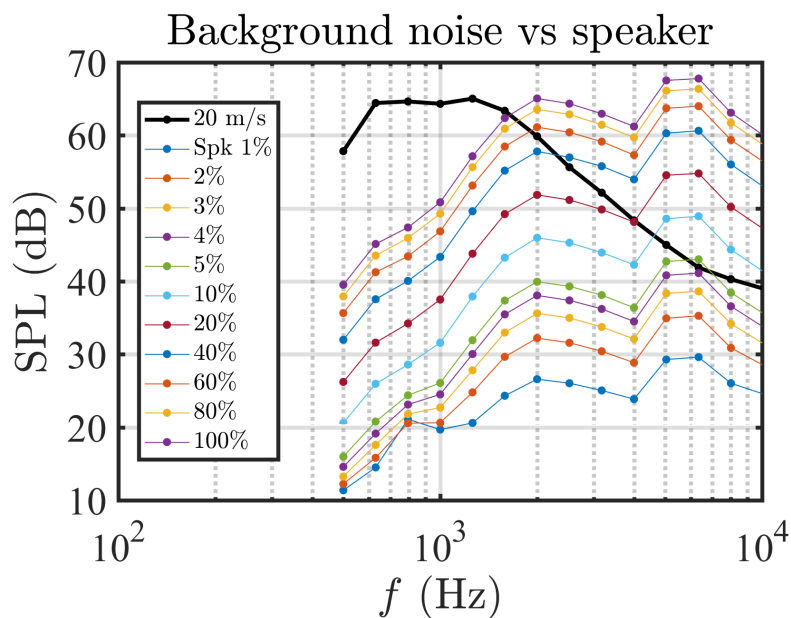


Figure 2: Background noise level (black) and speaker levels (color) that were used in the experiment.

3 Dereverberation Beamforming (DBF)

3.1 Description of the method

As the method has already been published, this section will only give the highlights of the DBF algorithm. For more details, please refer to [5].

In general, CBF is performed in the frequency domain, in which case the algorithm uses the CSM of the microphones data as an input. That CSM contains the whole information of the measured signal, including reflections if the test section is very reverberant. However, these reflections can not be directly visualised in the frequency domain, but they can be in the time domain. The idea is to apply an inverse Fast-Fourier Transform (FFT) on the CSM in order to get the Cross-Correlation Matrix (CCM) of the microphone signals. For a single monopole source, the CCM consists of an ensemble of cross-correlation functions, each of them containing a main peak (main source) and lower secondary peaks (reflections) at different time delays. All of these functions are then filtered around their main peak using a narrow Hanning window in order to remove the influence of the reflections. The last step consists in applying a FFT on the filtered CCM in order to recover a modified CSM.

A sketch of the DBF methodology is shown in Fig. 3

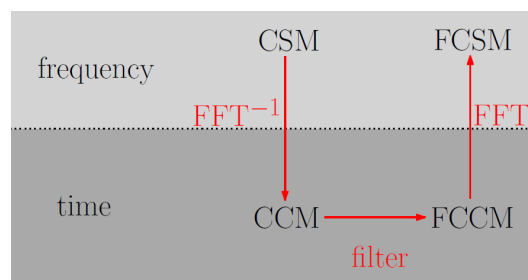


Figure 3: Summary of the DBF method.

3.2 Results

The authors first believed that the DBF method could recover the source location in the presence of a background noise, just as it already did in the case of a reverberant environment [5]. However, as the main source is now the fan, the peak on the cross-correlation functions must not be taken as the maximum (fan noise). Thus, the cross-correlation functions were filtered in a time-delay range corresponding to the actual source region. The latter is plotted in a black square in Figure 4(b), which shows the actual DBF result with the speaker at 10% at $f = 1587$ Hz (SNR=-10 dB). In the same configuration, CBF (Figure 4(a)) depicts noise on the right of the figure, where the fan is located. It can be observed that the effect of narrowing the filter around the source region in DBF does actually not help to recover the source, the sidelobes are just spread around the focusing region. That is why an alternative method was used to solve that particular problem, and the results are shown in the following.

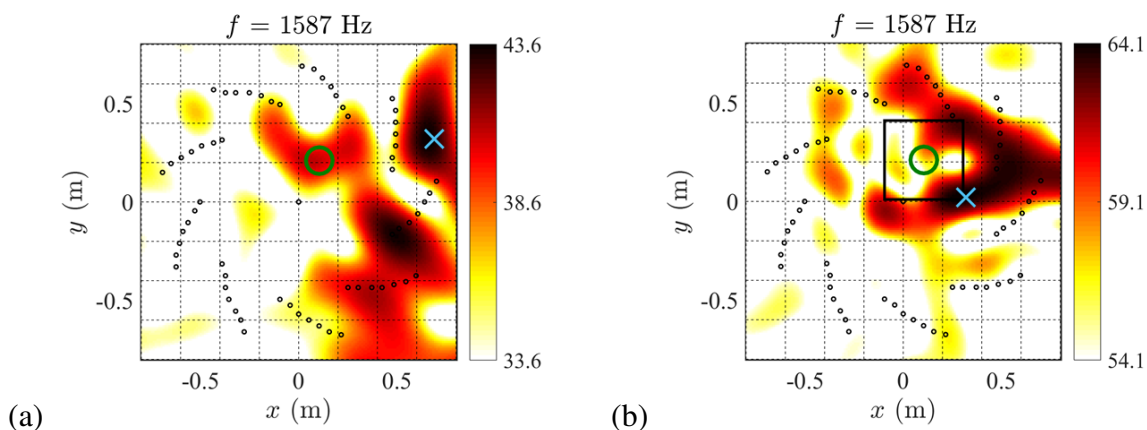


Figure 4: CBF (a) and DBF (b) on the speaker in flow case. The black box denotes the region for filtering the cross-correlation function. $f = 1587$ Hz and $U_\infty = 20$ m/s.

4 Eigenvalue Decomposition (EVD)

4.1 Description of the method

The EVD method proposed by Bahr and Horne [1] will be briefly described here, but more details can be found in the corresponding paper.

First, it is assumed that the measured CSM \mathbf{G} can be decomposed into the source CSM \mathbf{G}_s and the background CSM \mathbf{G}_d , which implies that the source and background noise are uncorrelated and that no coherent electromagnetic interference is present in the measurement:

$$\mathbf{G} = \mathbf{G}_s + \mathbf{G}_d. \quad (1)$$

Note that \mathbf{G} and \mathbf{G}_d are obtained from separate measurements. Then, an EVD is performed on the background CSM:

$$\mathbf{G}_d = \mathbf{X}_d \mathbf{\Lambda}_d \mathbf{X}_d^H, \quad (2)$$

where \mathbf{X}_d and $\mathbf{\Lambda}_d$ respectively denote the eigenvector and eigenvalue matrix of \mathbf{G}_d , and superscript H stands for the Hermitian transpose.

An operator \mathbf{B}_d is then defined:

$$\mathbf{B}_d = \mathbf{X}_d \mathbf{\Lambda}_d^{-1/2}. \quad (3)$$

However, before building that matrix, a threshold must be defined in order to remove the smallest eigenvalues (and corresponding eigenvectors) in $\mathbf{\Lambda}_d$. The choice of this threshold is very important as it can drastically change the resulting acoustic map.

The rest of the procedure is quite straightforward in the paper, so it will not be detailed here. The most important step is the choice of an optimal threshold when building \mathbf{B}_d .

4.2 Results

The influence of the threshold in EVD, mentioned in the previous section, is now discussed. Figure 5 shows the acoustic maps obtained after processing the EVD and while using three different thresholds in the eigenvalue matrix $\mathbf{\Lambda}_d$. It appears that if the threshold is too big (Fig. 5(a)), not enough information is provided and thus the source location is not found. On the other side, if the threshold is too small (Fig. 5(c)), the influence of the background noise becomes too important, leading to a dirty map. In the present case, a good compromise is found when the threshold is equal to 10^{-7} , as shown in Fig. 5(b). This value was used in the algorithm.

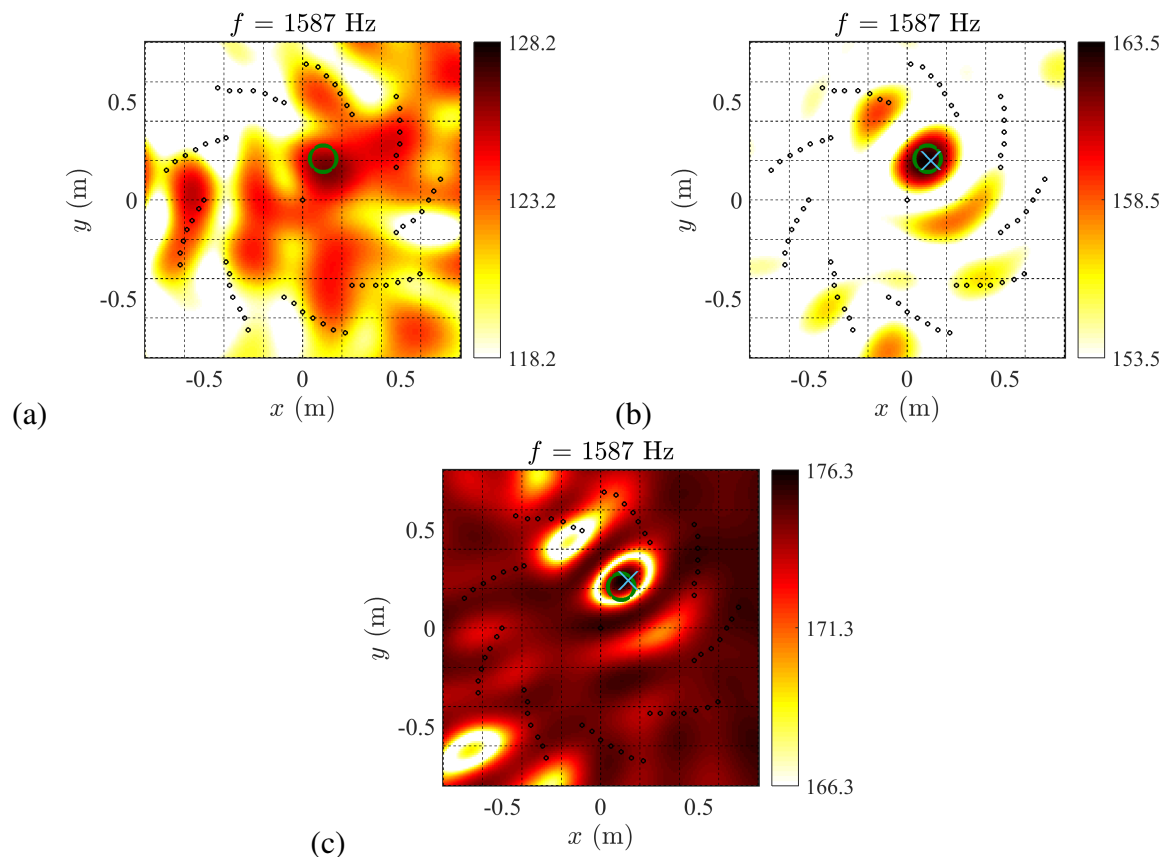


Figure 5: Acoustic maps obtained from EVD with different thresholds: (a) 10^{-5} , (b) 10^{-7} and (c) 10^{-9} . $f = 1587$ Hz and $U_\infty = 20$ m/s.

Some maps obtained through the EVD method are presented in Fig. 6 at the particular frequency $f = 1260$ Hz, as this frequency contains a few positive and many negative values of SNR. When the speaker is set to 4% (SNR=-22 dB), CBF is unable to recover the source location (Fig. 6(a)). However, EVD displays a map containing lots of sidelobes but with a maximum located at the speaker position (Fig. 6(b)). When the speaker is set to 20% (SNR=-8 dB), CBF still does not get the main source location (Fig. 6(c)) while EVD shows a main lobe where expected and small intensity sidelobes (Fig. 6(d)). These examples already show how efficient the EVD method can be. One remark concerns the level on the maps, which was wrongly recovered with EVD for some unknown reason.

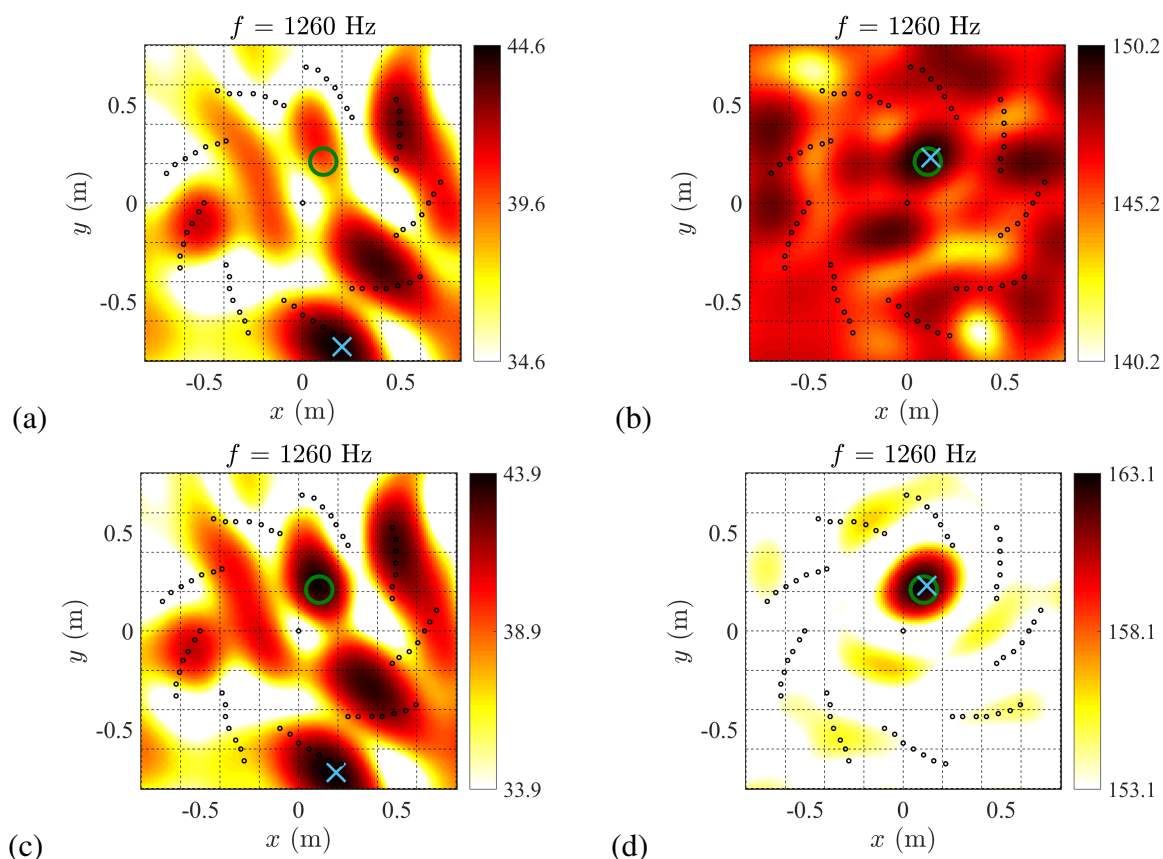


Figure 6: Comparison between CBF (left) and EVD (right) maps with speaker level at 4% (top) and 20% (bottom). $f = 1260$ Hz and $U_\infty = 20$ m/s.

The next step was to investigate the effect of EVD over the whole frequency range and for a big variety of SNR. This is shown in Fig. 7 where the location accuracy is displayed for all the speaker volumes and all the 1/3rd octave frequency bands. The values in red denote the SNR in each case, and white and black background respectively designate the cases where the source was and was not found at its expected location (with an error of 5 cm which corresponds to the speaker radius). It can be seen that EVD has mainly two effects: first, it helps to better recover the source location at low frequencies, from 1 kHz to 2.5 kHz. However, at higher frequencies the algorithm loses in accuracy and CBF is preferred. But overall, the lowest SNR at which sources can be detected changes from -22 dB with CBF to -42 dB with EVD, which is a noticeable improvement.

Some additional experiments were conducted in the same configuration, but without the speaker and with an airfoil in the test section. A NACA0012 with a chord of $c = 190$ mm was mounted on both sides of the inlet (2D configuration). It is untripped and has a 0° angle of attack. Figure 8 shows the CBF and EVD results for three 1/3rd octave frequency bands at which CBF was inefficient. For these three particular frequencies, CBF only catches the background noise from the fan, coming from the right, while EVD clearly detects trailing edge noise coming from the midspan. These results confirm the efficiency of the method in realistic aeroacoustic test cases.

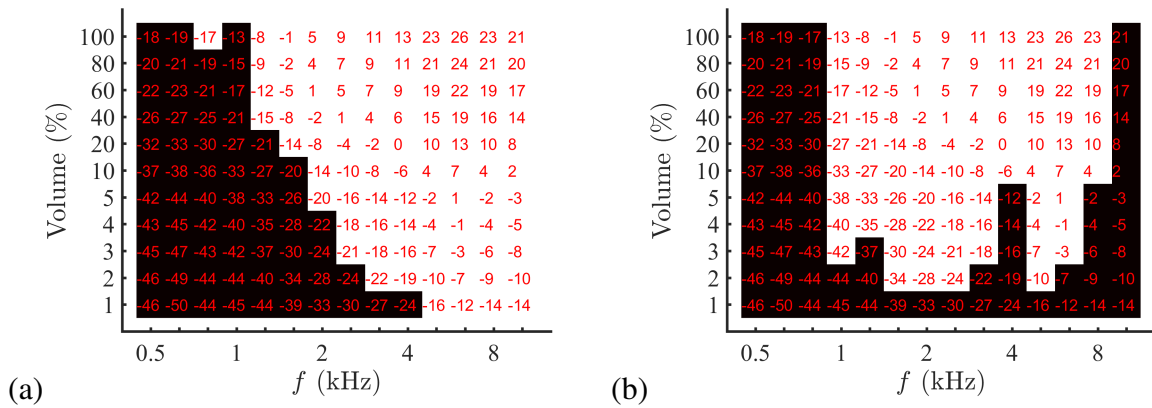


Figure 7: CBF (left) and EVD (right) location accuracy over the whole level and frequency ranges. White and black boxes respectively denote good and bad location estimation, and the values in red correspond to the SNR.

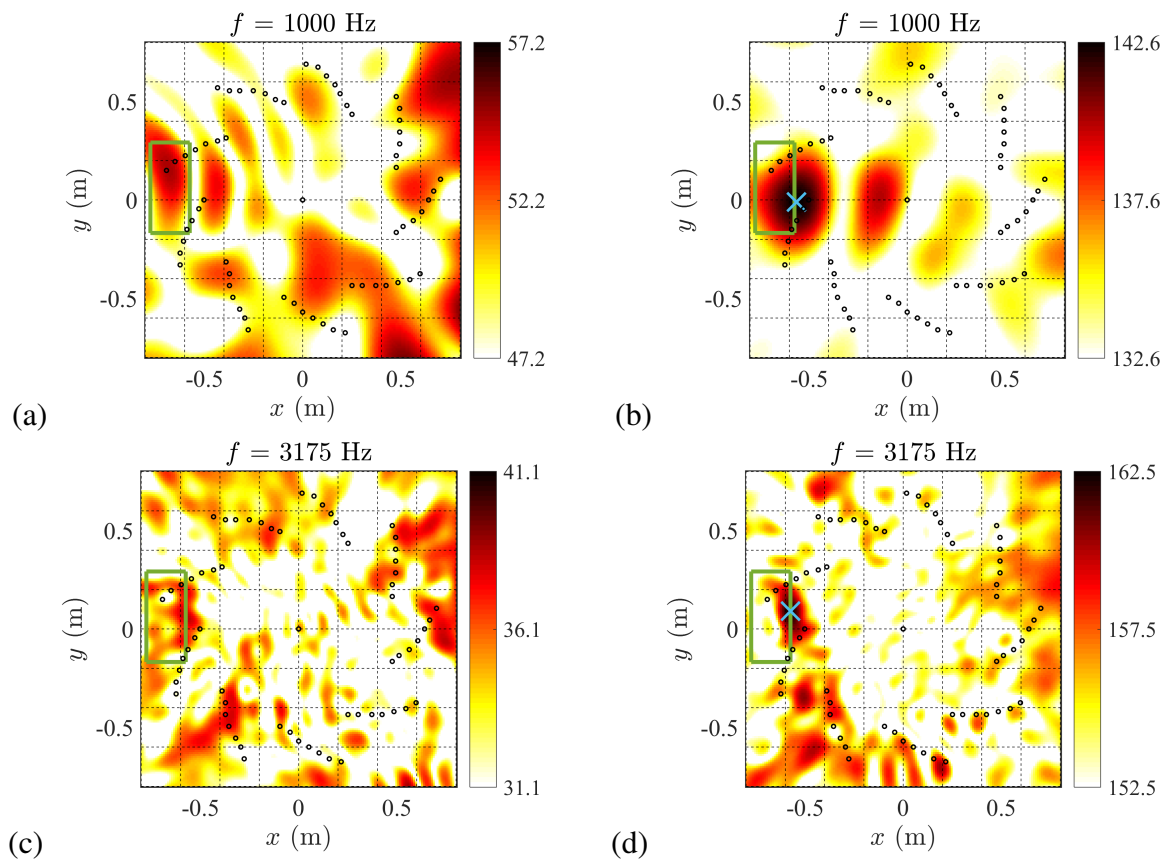


Figure 8: CBF (left) and EVD (right) results with the NACA0012 airfoil in flow at $f = 1000$ Hz (top) and $f = 3175$ Hz (bottom). $U_\infty = 20$ m/s.

5 CONCLUSIONS

This paper has presented two methods that were tested to improve beamforming results in respectively a high background noise environment.

The first one, DBF, was used because it has already shown great efficiency in the case of image sources due to a reverberant environment. However, even though DBF was modified to be adapted to the case of high background noise, no improvement could be found when compared with CBF.

Another technique was implemented, proposed by Bahr and Horne [1], and tested on both a speaker and an airfoil in flow. It was found that EVD could actually recover the source location with a twice lower SNR than for CBF. However, the level was badly recovered and the method is very sensitive to the threshold value choice.

This work as shown that there is still room for improvement in the field of aeroacoustic wind tunnel testings in noisy environments.

6 REFERENCES

REFERENCES

- [1] C. Bahr and W. Horne. “Advanced background subtraction applied to aeroacoustic wind tunnel testing.” In *21st AIAA/CEAS Aeroacoustics Conference, Dallas, Texas*, 3272. 2015.
- [2] B. Fenech and K. Takeda. “Towards more accurate beamforming levels in closed-section wind tunnels via de-reverberation.” In *13th AIAA/CEAS Aeroacoustics Conference, Italy, Rome*, 3431. 2007.
- [3] J. Fischer and C. Doolan. “An empirical de-reverberation technique for closed-section wind tunnel beamforming.” In *22nd AIAA/CEAS Aeroacoustics Conference, Lyon, France*, 2760. 2016.
- [4] J. Fischer and C. Doolan. “Beamforming in a reverberant environment using numerical and experimental steering vector formulations.” *Mech. Syst. Sig. Process.*, 91, 10–22, 2017.
- [5] J. Fischer and C. Doolan. “Improving acoustic beamforming maps in a reverberant environment by modifying the cross-correlation matrix.” *Journal of Sound and Vibration*, 411, 129–147, 2017.
- [6] S. Guidati, C. Brauer, and S. Wagner. “The reflection canceller - phased array measurements in a reverberant environment.” In *8th AIAA/CEAS Aeroacoustics Conference, Breckenridge, Colorado*, 2462. 2002.
- [7] L. Koop and K. Ehrenfried. “Microphone-array processing for wind-tunnel measurements with strong background noise.” In *14th AIAA/CEAS Aeroacoustics Conference, Vancouver, Canada*, 2907. 2008.
- [8] P. Sijtsma and H. Holthusen. “Corrections for mirror sources in phased array processing techniques.” In *9th AIAA/CEAS Aeroacoustics Conference and Exhibit, Hilton Head, South Carolina*, 3196. 2003.

- [9] T. Spalt, C. Fuller, T. Brooks, and W. Humphreys. “A background noise reduction technique using adaptive noise cancellation for microphone arrays.” In *17th AIAA/CEAS Aeroacoustics Conference, Portland, Oregon, 2715*. 2011.